Lab on a Chip

View Online
Dynamic Article Links

Cite this: *Lab Chip*, 2011, **11**, 863

www.rsc.org/loc

PAPER

A lab-on-chip for biothreat detection using single-molecule DNA mapping†

Robert H. Meltzer,* Jeffrey R. Krogmeier, Lisa W. Kwok, Richard Allen, Bryan Crane, Joshua W. Griffis, Linda Knaian, Nanor Kojanian, Gene Malkin, Michelle K. Nahas, Vyacheslav Papkov, Saad Shaikh, Kedar Vyavahare, Qun Zhong, Yi Zhou, Jonathan W. Larson and Rudolf Gilmanshin

Received 4th October 2010, Accepted 10th December 2010
DOI: 10.1039/c0lc00477d

Rapid, specific, and sensitive detection of airborne bacteria, viruses, and toxins is critical for biodefense, yet the diverse nature of the threats poses a challenge for integrated surveillance, as each class of pathogens typically requires different detection strategies. Here, we present a laboratory-on-a-chip microfluidic device (LOC-DLA) that integrates two unique assays for the detection of airborne pathogens: direct linear analysis (DLA) with unsurpassed specificity for bacterial threats and Digital DNA for toxins and viruses. The LOC-DLA device also prepares samples for analysis, incorporating upstream functions for concentrating and fractionating DNA. Both DLA and Digital DNA assays are single molecule detection technologies, therefore the assay sensitivities depend on the throughput of individual molecules. The microfluidic device and its accompanying operation protocols have been heavily optimized to maximize throughput and minimize the loss of analyzable DNA. We present here the design and operation of the LOC-DLA device, demonstrate multiplex detection of rare bacterial targets in the presence of 100-fold excess complex bacterial mixture, and demonstrate detection of picogram quantities of botulinum toxoid.

Introduction

The possibility of terrorist or criminal usage of bioagents as weapons has produced an urgent need for efficient detection and identification technologies.[1,2] Pathogen detection should be specific, sensitive, rapid, and with low false-positive rate. Biological pathogens include protein or peptide toxins, viruses, and bacteria that are so different in nature that currently each class requires different detection techniques. Universal detection of biological threats using a single instrument therefore represents a significant technical challenge.

The preferred approaches for detection of microbes are typically based on nucleic acid analysis and genotyping.[1,3] Among these techniques, Direct Linear Analysis (DLA) is especially suitable for detection of pathogenic bacteria.[4,5] Although DLA is not as sensitive as PCR, it has high specificity, does not introduce an amplification-based bias, is rapid, is capable of analyzing microbial mixtures, and does not require *a priori* knowledge (*i.e.* genomic sequence) about the targets.[5,6] Moreover, DLA implements a target-independent universal set of reagents for identification of a vast variety of targets in complex mixtures of bacteria.[4–6] In DLA, an isolated genomic DNA is specifically digested with restriction endonucleases and tagged with sequence-specific fluorescent probes. Individual DNA fragments are stretched by accelerated flow and interrogated one by one. Fluorescence of the DNA-bound probes is detected, and their positions on the DNA are determined. As the probes recognize short (8 nucleobase) sequences and DNA fragments used for analysis are long (100–250 kb), every fragment carries multiple probes. The specific pattern of fluorescent probe distribution on each DNA fragment is used for identification.

Although DLA could detect viruses with long double-stranded DNA genomes, such as *Variola major* (causing smallpox), it cannot detect small viruses carrying short and single-stranded genomes. DLA also cannot be applied to protein toxins, which represent major biohazards.[1,7] A novel suspension array was therefore developed based on a specialized recombinant DNA, called Digital DNA, that builds on the DLA principles.[8] Every Digital DNA carries specific antibodies or oligonucleotides to detect antigen or nucleic acid targets, respectively, similar to a sandwich immunoassay or a nucleic acid chip. A batch of Digital DNA molecules carrying a specific antibody or oligonucleotide also carries a unique fluorescent pattern used to identify the batch. Different Digital DNA batches are combined to form the suspension array, which is incubated with the sample and then interrogated using the same hardware as DLA.

Our Company is developing an air-sampling detector for continuous environmental monitoring. The heart of this system is a laboratory-on-chip, LOC-DLA. Previous demonstrations of DLA and Digital DNA detection have been performed on

US Genomics, 12 Gill Street, Suite 4700, Woburn, MA, USA. E-mail: rmeltzer@usgenomics.com

† Electronic supplementary information (ESI) available: Details of device design, performance, and data analysis. See DOI: 10.1039/c0lc00477d

isolated bacterial culture or on laboratory prepared immunoassays, respectively. LOC-DLA represents a novel application of these techniques to the stringent requirements of an environmental monitoring system. Specifically, this device has been designed to detect rare targets in low mass, mixed samples. The complex, monolithic lab-on-chip device described here includes features for on-chip sample concentration and length-dependent DNA fractionation to optimize the detection throughput. In this paper, we present the design of the LOC-DLA chip, describe procedures developed for its operation, and characterize the LOC-DLA performance. Although the chip, its structures, and protocols were developed for analysis of airborne samples, all aspects of the technology, taken in its entirety or as independent components, can be implemented for other tasks such as diagnosis of human infectious diseases or surveillance of food-borne pathogens.

Materials and methods

Reagents

Tris–borate–EDTA buffer (TBE, 45 mM Tris, 45 mM boric acid, 1 mM EDTA, pH 8.3) was purchased from Sigma Aldrich (St Louis, MO) as concentrated stock and diluted approximately 20-fold to obtain a conductivity of 270 pS. UltraTrol-LN was purchased from Target Discovery, Inc. (Palo Alto, CA), and used without further dilution. Solutions of 1 M NaOH, 40% acrylamide–bisacrylamide (19 : 1), hydroquinone, and 2-hydroxy-2-methylpropiophenone (Darocur 1173) were purchased from Sigma-Aldrich and used as received. The DNA was intercalated with POPO-1 (Invitrogen, Carlsbad, CA) at an intercalator-to-basepair ratio of 1 : 3.[5] Custom PNA tags were synthesized by Panagene (Daejeon, Korea) and labeled with the fluorescent dye ATTO550 (ATTO-TEC, Siegen, Germany).[4] All preparations were made using Ultrapure water (18 MΩ, Millipore, Billerica MA), filtered through a 0.2 μm filter immediately prior to use.

Bacterial culture and sample preparation

Our model targets were *Escherichia coli* (Gram-negative) and *Staphylococcus epidermidis* (Gram-positive) bacteria. The complex biological background was modeled by the mixture of *Brevibacterium epidermidis*, *Burkholderia gladioli*, *Bacillus muralis*, *Corynebacterium ammoniagenes*, *Flavobacterium johnsoniae*, *Paracoccus denitrificans*, *Rhizobium radiobacter*, *Stenotrophomonas maltophilia*, and *Vibrio fischeri*. See ESI† for details on bacteria culturing, sample preparation[9], and mixture composition. λ Phage DNA (48.5 kb, accession #NC_001416) was purchased from New England Biolabs (Ipswich, MA). BAC 12M9 DNA (185.1 kb, accession #AL080243) was prepared as described before.[10]

Design and fabrication of the lab-on-chip

The LOC-DLA microfluidic chip (Fig. 1) was fully designed and developed at US Genomics. The chips were manufactured by Micralyne, Inc. (Edmonton, Alberta, Canada) using wet-etch and deep reactive ion etch (DRIE) techniques. Chips were bonded to custom-designed polymethylmethacrylate (PMMA) manifolds (Eastern Plastics, Bristol, CT) at US Genomics using a UV-curable adhesive Dymax 140M (Dymax Corporation, Torrington, CT). See ESI† for further details.

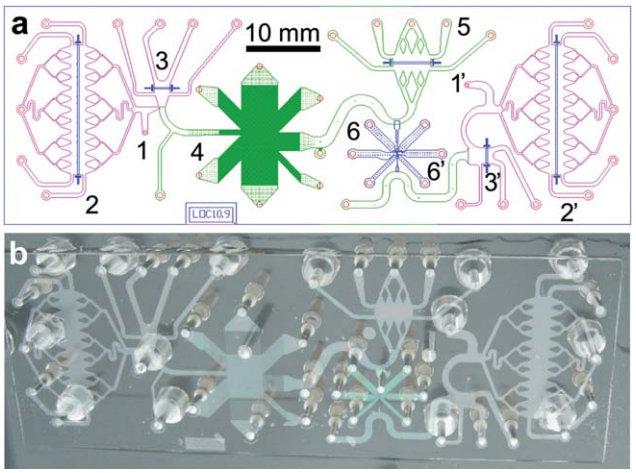

Fig. 1 Schematic drawing of laboratory-on-chip, LOC-DLA, (a) and picture of its assembly with manifold (b). Features etched to the depths of 20 μm, 2 μm, and 1 μm are presented with pink, green, and blue lines in schematic, respectively. The functional components include: 1, DNA injection port; 2, primary DNA concentrator; 3, secondary DNA concentrator; 4, DNA prism fractionator; 5, tertiary DNA concentrator; 6, DNA stretching microfluidics. Corresponding functional components of the Digital DNA portion of the device are labeled 1′–6′. Blue lines across the structures 2, 3, and 5 indicate 1 μm deep features superimposed with 2 or 20 μm deep channels.

Fabrication of photopolymerized polyacrylamide gels

Polyacrylamide gels were fabricated *in situ* in LOC-DLA to serve as DNA concentrators.[11] Briefly, the chip was filled with a solution of acrylamide-bisacrylamide and photoinitiator. Gels were polymerized at appropriate positions (Fig. 1a, features 2, 3, and 5) by scanning the chip mounted on a motorized XY translation stage past a 335 nm light source on an inverted microscope. Residual non-polymerized monomer solution was then evacuated from the chip by thorough flushing with water and TBE. See ESI† for detailed fabrication methods.

Fig. 2a indicates the structure of the primary concentrator on LOC-DLA. The photopolymerized gel bank was fabricated centering on a 1 μm deep etched feature (blue) superimposed on a 20 μm deep channel, which was used to mechanically lock the gel in place. The polymerized gel and alignment fiducial marks are shown in Fig. 2b.

Surface treatment

The control of electroosmotic flow (EOF) is required for fast and reliable electrokinetic transfer of DNA in microfluidic devices. As EOF is driven by interactions of ions with external electric field and surface charge, surface treatment is critically important to control EOF, especially in fused silica chips in shallow 1–2 μm deep areas.[12,13] After extensive investigation, we chose Ultra Trol-LN as an EOF suppressant for its reproducible behavior, excellent EOF suppression, and the ability to regenerate previously used devices through multiple rounds of recoating.

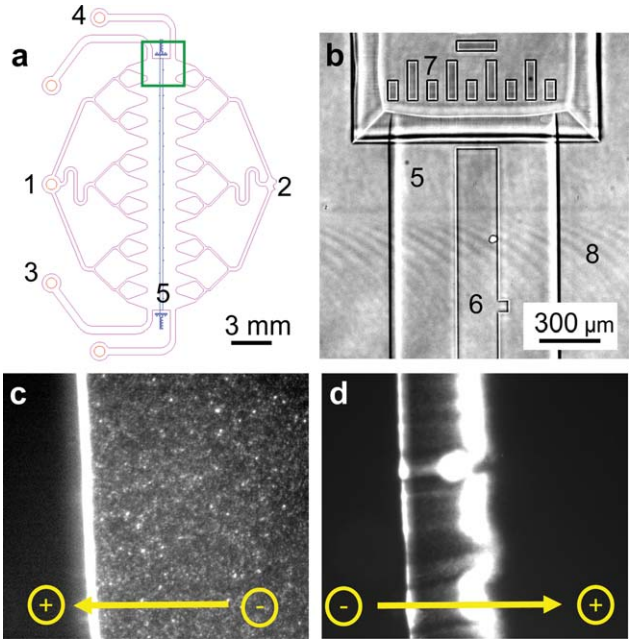

Fig. 2 Polyacrylamide gel bank fabricated within LOC-DLA. (a) Schematic of the primary concentrator (feature 2 in Fig. 1). Ports 1 and 2 were used for electrodes. Ports 3 and 4 were used for hydrodynamic access for gel formation, flushing, and control of ion depletion behind the gel bank. Retaining trench, 5, was used for gel bank positioning. (b) A bright field image of polymer bank fabricated within the chip cavity as indicated in green square in Fig. 2a. Polymerized gel, 5, is held by retaining trench, 6. Also marked are alignment fiducials, 7, and buffer-filled volume, 8. (c) The fluorescence image of DNA concentration on the gel surface. The BAC DNA (1 μg μL^{-1}) was introduced through port 2 and concentrated at 25 μA (~15 V cm^{-1}) over several minutes. Individual DNA molecules are observed as discrete fluorescent points to the right of the gel. The bright band indicates accumulation of DNA at the gel surface. (d) The fluorescence image of DNA elution from the gel surface. After DNA concentration, the electrode polarity was reversed, and the DNA was eluted from the gel surface at 3 μA. The DNA elutes as a concentrated band.

The treatment on LOC-DLA began by priming with water followed by an injection of 0.1 M NaOH solution to clean and activate the fused silica surface. After flushing thoroughly with water to remove the residual NaOH, the channels were filled with UltraTrol-LN solution and incubated at room temperature for at least 30 minutes. We found that excess coating of UltratTrol caused sticking of DNA to the fused silica surfaces, likely through non-specific electrostatic interactions. To eliminate this effect and maximize DNA electrophoretic mobility (data not shown), the entire device was flushed with 0.2 M NaCl solution. Prior to operation, the device was washed thoroughly with water and then with TBE buffer. The described procedure ensured an EOF suppression over 5–6 consecutive runs, after which the device was regenerated by repeating the NaOH, water, Ultratrol, and NaCl flushing sequence.

Control and automation of operation

For the control of LOC-DLA, Oztek (Merrimack, NH) built a custom, multi-electrode high-voltage power supply that permitted independent operation of up to 12 discrete electrodes, with applied voltages up to 2 kV. This power supply also incorporated on-board current sensors accurate to 0.1 μA. Automated pressure regulators (Alicat Scientific, Tucson, AZ) maintained pressure in seven independent zones under computer control. TBE-filled Tygon tubes connected the manifold-bonded microfluidic device to a series of wells integrated into a remote assembly. This assembly, in turn, was interfaced with the pneumatic and electrical control hardware. This interface was used to control the voltage and pressure of each port on LOC-DLA, while eliminating bubble formation in micron-scale chip features due to electrolysis at the electrode (see ESI† for details).

The high voltage power and pressure were controlled by National Instruments (Austin, TX) hardware and custom software running on a Windows PC. This software allowed for hands-free automated operation of LOC-DLA. Multi-stage protocols with unique electrode pairings, applied voltages, durations, and pneumatic states could be combined using the custom GUI. The software also performed automated calibration of the electrical resistance of the fluidic pathways throughout the LOC-DLA device. Pre-calibration of LOC-DLA was required prior to every run to correct for subtle differences in the buffer conductivity, instrument-to-instrument variability, and LOC-DLA etching variability.

Protocol development and testing

We characterized electrokinetic transfers by direct observation of DNA migration using fluorescence microscopy. The protocol development experiments were performed using λ phage DNA intercalated with POPO-1 at a 3 : 1 base pair-to-intercalator ratio; 5 μL samples at 1 ng μL^{-1} DNA concentration were introduced by a pipette into the LOC-DLA injection port. The DNA was transferred electrokinetically at constant voltages to achieve a desired current (see ESI† for the transfer procedure).

DNA molecules within the chip were observed using an inverted fluorescence microscope Eclipse TE 2000-S with a 10× Plan Fluor objective, 0.74 NA (Nikon, Tokyo, Japan). Fluorescent images of the intercalated DNA were detected using a CFP-2432A_NTE-zero spectral filter (Semrock, Inc., Rochester, NY) and a SensiCam qe CCD camera (Cooke Corporation, Romulus, MI). DNA transfer times were measured by monitoring the arrival of DNA at designated landmarks on the chip. The transfer time was defined as the time during which 90% of DNA had passed the point of inspection. At least 5 observations of each step were used to estimate DNA transfer times. Protocols for stretching of DNA in microfluidic funnels were previously developed and presented.[5,14]

Direct linear analysis—data acquisition

DLA measurements were performed as previously described.[5,8,14] Briefly, DNA molecules were stretched to near contour length by accelerated flow formed by a two-dimensional funnel. Once extended, the DNA molecule passed through three spots of focused laser light. In two spots, the light with 445 nm wavelength excited fluorescence of the intercalated DNA backbone, and in the third spot, the light with 532 nm wavelength excited the ATTO550 fluorophores of bisPNA tags hybridized to specific

sites along the DNA molecule. The resultant fluorescence from the three spots was confocally detected in three corresponding detection channels. The fluorescence signal in the two channels detecting DNA backbone fluorescence provided information about the velocity and length of individual DNA molecules, and the signal generated by specific tags was used to map their locations on the extended DNA backbone.

DLA was performed using a custom acquisition system that provided fully automated positioning of the LOC-DLA device relative to the illumination and detection optics. As a control, DLA of the DNA samples was also performed using a simple, fluidics-only chip that lacked concentration and fractionation functions. This device has been described previously.[5,8] These data were used to evaluate the effect of sample concentration and fractionation on information throughput in LOC-DLA.

Direct linear analysis—data analysis

In the first stage of DLA data analysis, the *GeneEngineer* software[10,14] was used to identify single molecule traces. Fluorescent signals in the tag channel were correlated with corresponding events in the two intercalator signal channels, and these molecule traces were exported for further analysis. *GeneEngineer* analysis also provided information about the length and velocity distributions of observed fragments.

Interpretation of the site-specific fluorescent tagging was achieved by either clustering similar fragments or evaluating single molecule fluorescence traces by comparing them to a database of empirically or theoretically predicted templates. The clustering algorithm has been described previously[5] and was used for the identification of simple mixtures of bacteria. Template-based matching was required for analysis of complex mixtures of bacteria, where the target of interest was mixed with a large proportion of background DNA molecules. Details of the template-based classification method are presented in the ESI†.

Results

LOC-DLA concept and operation

LOC-DLA is a complex device designed to perform two distinct assays: Direct Linear Analysis of genomic DNA from bacteria and non-bacterial pathogen detection using the Digital DNA suspension array. From a collected air sample, bacteria were separated from smaller viruses and small molecule toxins by centrifugation in a density gradient. Both sample types were then prepared in parallel using automated mini-reactors.[4,8] From there each sample type is processed separately in physically isolated fluidic circuits on the same chip. Both sections utilize photopolymerized polyacrylamide gels to electrokinetically concentrate the prepared DNA samples from the ~100 μL volume delivered from the mini-reactor into the ~10 nL volume required for DLA. Likewise, both structures incorporate microfluidic funnels for DNA extension and analysis. The DLA portion of the device also requires length-based fractionation of the genomic DNA for optimal throughput and efficiency and, therefore, includes the DNA prism, which is absent in the Digital DNA section of the device. The structural features of LOC-DLA are detailed in Fig. 1, for a schematic of the detector workflow, see ESI†.

The basic operation sequence of LOC-DLA for bacterial genomic analysis begins with injection of a sample containing approximately 5 ng of prepared DNA into the injection port (Fig. 1a, feature 1). When directly coupled to the automated sample preparation mini-reactor, the eluted volume is approximately 100 μL. Alternatively, 5 μL of a prepared sample can be manually delivered directly into the injection port. This sample is then concentrated at the first polymer gel bank (feature 2) at 25 μA for 45 minutes, and then further concentrated at the secondary gel bank at 3 μA for 45 minutes (feature 3). The sample is then eluted from the secondary gel bank toward the DNA prism at 1 μA for 3 minutes and then processed through the prism (feature 4) for 45 minutes. Here long DNA fragments are isolated and collected at the final gel bank (feature 5). The concentrated long fragments are then eluted from the final gel at 0.4 μA for 3 minutes and positioned near the DLA stretching channel (feature 6). The DNA stretching and molecule-by-molecule DLA measurement are then performed under hydrodynamic control at ~10 psi vacuum, typically for a one hour acquisition. (See ESI† for a graphic illustration of the LOC-DLA operation sequence.)

For toxin detection, the opposite side of the LOC-DLA is used, which includes two concentrating gels and stretching fluidics comparable to the respective structures of the DLA side (Fig. 1a, features 1′–6′). This assay uses an engineered Digital DNA of uniform, predetermined length. Fractionation is therefore not required to eliminate short DNA fragments. The detection funnel on the Digital DNA section of the device is optimized for stretching shorter DNA fragments than are used in DLA.

The core functions of sample concentration and DNA fractionation were optimized in stand-alone prototype devices prior to their integration in LOC-DLA. Interfacing the individual components introduced additional constraints to the functional design of the device to minimize the volume between sequential stages and to minimize the loss of DNA in the eluted bands due to field bending or tailing effects. Here, we first describe implementation and optimization of DNA concentration and fractionation, and then demonstrate the integrated function of LOC-DLA. We do not elaborate on microfluidic DNA stretching, which has been presented in detail previously.[10,14]

Polymer gel DNA concentrators

Photopolymerized acrylamide gels serve two important functions in LOC-DLA. First, they concentrate the DNA delivered from the sample preparation system. Second, the gel surfaces also serve as hard stops along the path of electrokinetic DNA transfer, which help to transform loose "clouds" of DNA into tight bands, thus minimizing operation timing. The gel banks concentrate the DNA by acting as semi-permeable barriers; small ions flow freely through the gel while the DNA accumulates at the surface. Directing the DNA towards and away from the gel surface is accomplished by an electric field controlled by electrodes placed before and behind the gel (Fig. 2). By placing a cathode behind the gel surface and an anode at the DNA injection port (Fig. 2a), negatively charged DNA is driven toward the gel surface where it accumulates (Fig. 2c). By

reversing the electrode polarity, the DNA can be eluted from the gel surface, resulting in a tightly concentrated band (Fig. 2d). Uniform distribution of DNA across the gel surfaces requires a uniform electric field distribution across the gel surface. This behavior was achieved by splitting the DNA stream into multiple serpentine channels in front of the gel face and using triangular diffusers, particularly at the primary and tertiary concentrators (Fig. 1, features 2 and 5; see ESI† for additional detail).

We observed that if the concentration step was performed at a fixed voltage, the current across a gel dropped significantly, leading to a decreased DNA mobility. This decrease was due to ion depletion in the buffer behind the gel.[15] To maintain a constant current at a given voltage, the backside of the gel must be flushed (using ports 1 and 3 in Fig. 2a) with fresh TBE buffer continuously during operation (see ESI†). We also found that the electric field in the chip must be limited to avoid damage of long DNA molecules and to prevent degradation of surface coatings. The electric field in the device was limited to 15 V cm^{-1} at the surface of gel banks and 300 V cm^{-1} in the channels. These field constraints in turn limited the velocity of DNA (V_{DNA}) during electrokinetic transfer, which is given by $V_{DNA} = \mu E$, where μ is the electrophoretic mobility of DNA and E is the electric field.

To maximize the speed of transfer of DNA in a compact, uniform band from the injection port to the entrance of the DNA prism, two gel banks were used to perform sequential DNA concentration. The 18 mm primary gel bank accommodated the initial sample concentration at 25 μA. This allowed for rapid transfer of DNA through the long distance from the external reactor. This concentrated band of DNA was then transferred toward the 2.3 mm secondary gel at 3 μA. Initial designs of LOC-DLA with only a primary gel resulted in significant band dispersion in transit to the DNA prism, and correspondingly longer prism operation times.

Retention of DNA at the polymer gel surface was a concern and a potential source for the loss of DNA in the chip. In fact, as much as 19 ± 8% of a 1 ng sample was retained at the primary concentrator surface. This phenomenon can be observed in Fig. 2d where fluorescence signal can be seen at the gel surface while the majority of the concentrated DNA is eluted electrokinetically. DNA retention at the gel has been addressed in several ways. First, the composition of the gel monomer solution was carefully selected to minimize DNA retention and optimize gel longevity. Second, gels were passivated by pre-running the chip with a sample of λ-DNA in an attempt to fill voids in the gel surface with the sample DNA that could be easily distinguished from the tagged bacterial DNA. Finally, the retained DNA was removed from the device by exposing the chip to the light with 333 nm wavelength between runs, thus photoscissioning any remaining DNA down to the size that could be removed and eliminating carryover from one run to the next in serial operation of the LOC-DLA device.

Fractionation of genomic DNA by length

The "DNA prism" was first described by Huang *et al.*[16] as a microfluidic device capable of high throughput, continuous, length-based fractionation of mixtures of long DNA molecules. Similar to the published work,[17] our device (Fig. 3a) is comprised of an array of micron-scale posts arranged in a two-dimensional hexagonal array. This postarray is surrounded by eight fluidic resistor banks to apply uniform electric fields with specified amplitudes and orientations within the array. DNA molecules migrate within the prism in the direction of the applied electric field. Oscillating the field between angled (E_1) and horizontal (E_2) orientations with appropriate field strength and duration results in angular separation between long and short DNA fragments.

In the angled phase (E_1), long and short fragments co-migrate between rows of posts. As the electric field re-orients 120° to the horizontal phase, DNA molecules are forced through a postline. When a coiled molecule of DNA interacts with a post, it extends or hooks across one or more posts and then slides in the horizontal direction. With the correct prism timing cycle, long DNA molecules remain trapped on their posts while shorter fragments disengage and migrate freely in the horizontal orientation. When the field reorients again to the angled phase, long molecules return to their original track, while shorter fragments migrate in parallel, but shifted laterally into neighboring rows. Over many repetitions, this behavior results in an angular separation between streams of long and short fragments (Fig. 3b). Careful design of the exit port geometry allows for shorter molecules to be directed towards a waste port, while longer fragments are retained for further analysis. In LOC-DLA, this occurs by collecting the isolated long fragments at a polymer gel concentrator (Fig. 1a, feature 5).

Efficient implementation of DLA requires removal of DNA fragments shorter than 150 kb (see ESI† for discussion). Starting with the DNA prism geometry previously described[16] as a baseline, we adjusted both geometric and operational parameters to achieve this desired fractionation. We explored postsize, interpostspacing, etch depth, electric field intensity, cycle timing, buffer composition, and surface treatment. Optimization of the prism geometry was performed in a series of standalone prototypes cast in polydimethylsiloxane (PDMS). From these studies, a device that achieved the best isolation of DNA fragments longer than 150 kb had 5 μm posts separated by 10 μm center-to-center distances in a hexagonal grid and etched to 2 μm depth (Fig. 3b). This geometry was reproduced in the LOC-DLA design. The timing for optimal fractionation is specific for each post-field geometry and was determined experimentally. The operation cycle found to yield the best separation in the final device includes three phases: (1) 80 V cm^{-1} angled field for 450 ms (E_1), (2) 0 V cm^{-1} relaxation phase for 100 ms, (3) 80 V cm^{-1} horizontal field for 280 ms (E_2).

The length-dependent DNA fractionation was demonstrated in LOC-DLA experimentally using a series of engineered DNA fragments of uniform lengths ranging from 125–165 kb. Representative composite images of DNA streaming through the LOC-DLA prism are shown in Fig. 3c. To monitor DNA separation in the prism, homogeneous samples of intercalated DNA of 125, 145, or 165 kb length were imaged under 10× magnification at 50 ms intervals and summed over a 10 s acquisition. Up to four fields of view were collected for each tested DNA population, and composite images were generated spanning a distance of up to 3 mm across the exit channels of the prism. In these images, the retained and waste channels of the DNA prism were visible. DNA migrating in the device appears as a bright cloud with zigzagging bright lines indicating the time-averaged trajectory of individual DNA particles. For 165 kb

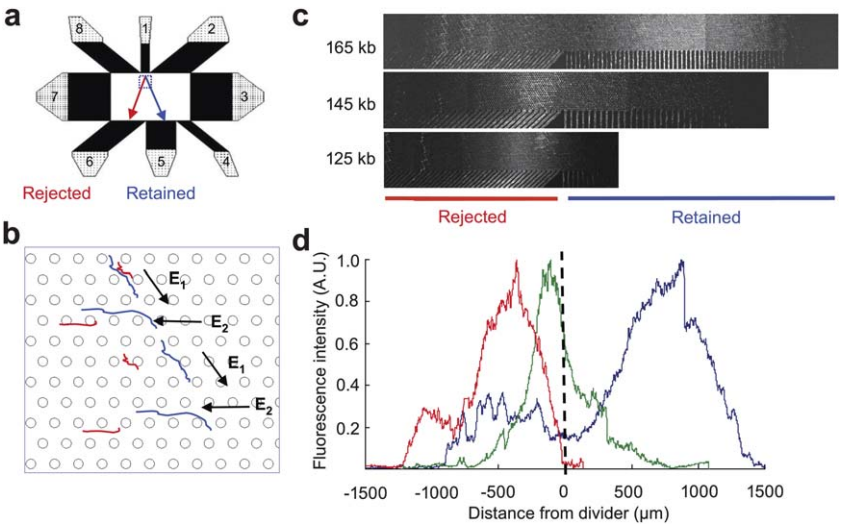

Fig. 3 Length-based DNA fractionation in DNA prism. (a) Schematic of the DNA prism (rotated by 90° relative to the in-chip orientation in Fig. 1), comprised of postfield (white square) connected by fluidic resistor channels (black parallelograms) with electrode ports (1–8). DNA enters through port 1 and exits through ports 6 (rejected short fragments) and 5 (retained long fragments). (b) A section of the postarray enlarged for clarity. Posts are 5 μm in diameter with 10 μm spacing center-to-center. Short (red) and long (blue) molecules are depicted migrating in the postarray with alternating electric field orientations E_1 and E_2 as described in the text. Images (c) and position histograms (d) of different length DNA molecules exiting the prism. Dashed line at the zero coordinate corresponds to the separation between channels leading to ports 2 and 4. The experiments were performed with 165 (blue), 145 (green), and 125 kb (red) homogeneous DNA samples (blue, green, and red histograms, respectively). Separation was performed with the following repeated electric field sequence: angled field 80 V cm^{-1}, 450 ms, pause 100 ms, horizontal field 80 V cm^{-1}, 280 ms.

DNA, the majority of the DNA particles migrated toward the retained port, with a minor component shunted to waste. We confirmed independently by gel electrophoresis characterization that the engineered DNA samples included a variable, sometimes substantial fraction of shorter molecules (see also the shoulder in the histogram for 125 kb DNA). Compared to the behavior of the 165 kb fragment, the 145 kb fragment appears to straddle both the retained and waste ports, while the 125 kb fragment is completely directed towards the waste channel. Fig. 3d shows the fluorescence intensity of a line cut from the previous micrographs relative to the central split between retained and waste ports. The comparison among 125, 145, and 165 kb fragments clearly indicates the differential migration of these species in the DNA prism under optimal conditions. Discontinuities in the intensity plots correspond to interfaces between component frames in the composite images, varying due to the brightness distribution of the illumination source of the microscope. These results demonstrate fine length-dependent separation in the LOC-DLA prism, with the size cutoff near 150 kb.

Integrated LOC-DLA operation for bacterial identification

To evaluate the effect of concentration and fractionation on the information throughput of DLA, we compared DLA of a simple mixture of bacterial genomic DNA using the LOC-DLA device and a simple fluidics-only chip[4,5] (general use chip, GU) that lacks concentration and fractionation functions. The sample contained a 9 : 1 mixture of *E. coli* and *S. epidermidis* whole genomic DNA digested with the restriction enzyme ApaI and tagged with bisPNA tags complementary to the sequence GAGAAGAA. The ApaI digest of *E. coli* and *S. epidermidis* produced 66 and 37 individual DNA fragments, respectively. Of these, *E. coli* and *S. epidermidis* had 7 and 3 fragments, respectively, between 150 and 250 kb, the ideal range for DLA (see ESI† for restriction maps). LOC-DLA was loaded with 5 μL of prepared DNA diluted to 100 pg μL^{-1}. A similar mass load was expected in collected air samples on the integrated detector. The GU device was loaded with 5 μL of undiluted prepared DNA at 1 ng μL^{-1}. This higher sample concentration was required for the GU chip to compensate for the lack of acrylamide gel concentrators. Without on-chip concentration, sample detection time becomes unmanageable at the load delivered to the LOC-DLA device.

Fig. 4a and b show the presence of the detected DNA fragments of different lengths.[5,14] In this two-dimensional histogram (heat map), the average backbone fluorescent intensity is plotted *versus* the observed molecule length for every detected molecule. Molecules with similar lengths cluster into punctate groups. In the GU run, fragments ranging in length from 0 to 100 μm are apparent (Fig. 4a). When the sample was fractionated on LOC-DLA prior to DLA, molecules shorter than 45 μm (or 135 kb) were removed (Fig. 4b). Some very short events remain near the origin of the molecule distribution plot. Due to the low observed intensity and very short observed length, these events are likely fluorescent admixtures (dust) and artifacts of the molecule identification algorithm due to signal noise in the blue detection channels.

Due to high-density, sequence-specific tagging, the information-rich generated patterns allow for precise discrimination between DNA fragments. Even fragments with very similar lengths, such as a 222 kb *E. coli* fragment and 223 kb *S. epidermidis* fragment observed in the same sample on LOC-DLA, are easily distinguishable (Fig. 4c). In this sample, 1839 *E. coli* molecules and 506 *S. epidermidis* molecules were

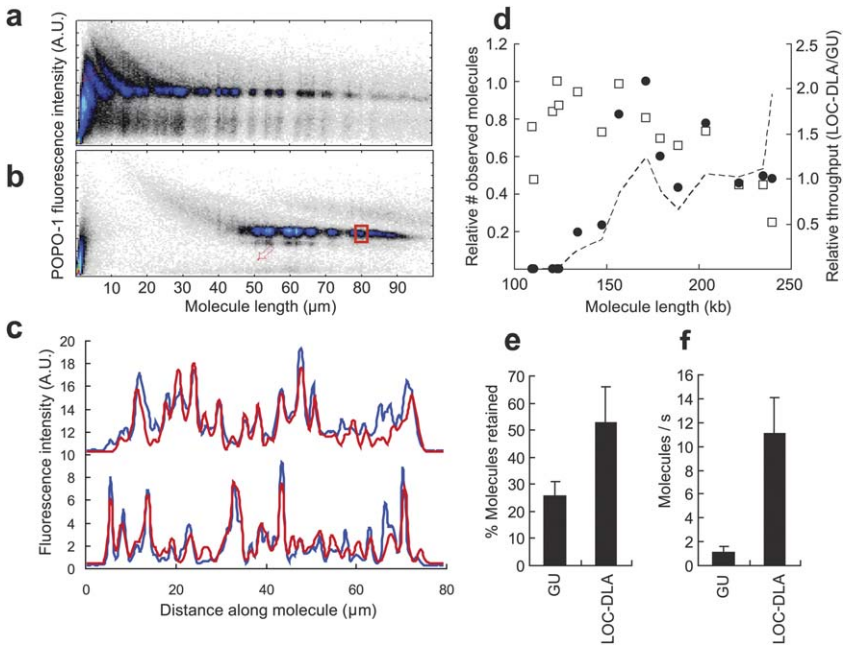

Fig. 4 Comparison of the performance of microfluidics-only general use chips (GU) and LOC-DLA using the same sample of 9 : 1 mixture of *E. coli* and *S. epidermidis* genomic DNA (see text for detail). Distribution of molecules detected on GU (a) and LOC-DLA (b). For each molecule, average backbone signal intensity is plotted *vs.* observed fragment length. (c) Observed tagging patterns for 222 kb *E. coli* fragment (bottom) and 223 kb *S. epidermids* fragment (top) obtained in LOC-DLA. Molecules were selected from red box in (b). Experimentally determined signal (blue) compared to the theoretical template (red) for both fragments. Average fluorescence intensity is plotted *vs.* distance along the linearized molecule (μm). (d) Relative molecule throughput (left axis) of all fragments observed on GU (open squares) and LOC-DLA (filled circles). For each sample, the molecule count is normalized to the most frequently detected fragment. Ratio of fragments observed on LOC-DLA *vs.* GU is shown in dashed line (right axis). (e) Proportion of non-overlapped DNA molecules detected with GU and LOC-DLA. Averaged from $n = 5$ paired experiments. (f) Detection throughput (the number of molecules detected per second) with GU and LOC-DLA. Averaged from $n = 5$ paired experiments.

identified. Furthermore, the tagging pattern for DNA fragments observed on LOC-DLA matches sequence-derived theoretical templates (Fig. 4b, generation of theoretical templates has been described previously).[4,5]

The potential loss of bisPNA probes during the electrokinetic transfer of tagged DNA throughout LOC-DLA was a concern. If dissociated, positively charged probes would effectively be separated from negatively charged DNA in the presence of an electric field. Using the clustering algorithm, we observed that the average tagging pattern in samples processed on LOC-DLA and GU was identical for common fragments (data not shown). For all molecules ranging from 50–58 μm (~135 to 157 kb) 8.94 ± 3.12 tags were observed on each molecule when run on GU and 7.6 ± 3.03 tags were observed on each molecule on LOC-DLA. Therefore, DNA tagging was preserved on LOC-DLA.

Using further clustering analysis, all *E. coli* fragments were identified in both GU and LOC-DLA datasets with fragment lengths ranging from 100–250 kb (Fig. 4d). The use of the clustering algorithm allowed for positive matching of identical fragments in both datasets despite small differences in the stretching behavior of the different chips. Only *E. coli* fragments were included in this analysis, because *E. coli* was the dominant species in the sample and the *E. coli* genome generated many fragments throughout the whole length range. Each fragment generated by restriction digest of a single species is expected to be present at uniform stoichiometry. For the case of either the GU or LOC-DLA data, the observed number of molecules for each fragment generated by the ApaI restriction digest was normalized to the number of the most frequently observed fragment. The sample run on GU showed that fragments with lengths ranging between 120 and 204 kb were observed with nearly the same frequency. Fragments longer than 204 kb appeared less frequently, limited by the tendency of longer molecules to overstretch in the DLA funnel under the measurement conditions.[14] On LOC-DLA, the number of fragments shorter than 156 kb gradually decreases to zero. Longer fragments are present at ratios similar to those observed in GU. These data demonstrate a DNA retention cut-on near 150 kb.

To compare the molecule detection throughput in LOC-DLA and GU, we conducted a series of five direct comparisons using separate matched samples, each measured in both devices. Samples were run at their prepared concentration of 1.8 ± 0.8 ng μL^{-1} on the GU devices. On LOC-DLA, these samples were diluted to 1 ng μL^{-1}. 5 μL were loaded on each device. Overlapping molecules were identified using their backbone fluorescence profile[5] and excluded from further analysis. Samples run on the GU chip had only ~20% non-overlapping molecules. On LOC-DLA, the percentage rose to ~50% despite running at much higher linear molecule concentration (Fig. 4e). Qualitatively this result is expected, because the probability of overlapping fragments increases with concentration of molecules and the LOC-DLA sample after fractionation contains fewer *molecules* at the same *mass* concentration (see ESI†). The throughput of non-overlapped molecules in the GU samples was

1.1 ± 0.6 molecules per second. Because of higher observed DNA *molecule* concentration and a reduced rate of molecule overlap due to smaller proportion of short fragments, the throughput on LOC-DLA was 11 ± 3 molecules per second, effecting a 10-fold improvement in information throughput, despite being loaded at lower concentration and total mass on LOC-DLA compared to GU (Fig. 4f).

Bacterial identification in complex mixture

To assess the capability of LOC-DLA to implement DLA for detection and identification of bacterial targets in mixtures, we prepared a representative model of a complex biological background, as expected for an environmental air sample (see Materials and Methods and ESI† for details). Our model targets, *E. coli* (10^4 cells corresponding to 50 pg of DNA) and *S. epidermidis* (10^5 cells corresponding to 250 pg of DNA), were spiked into an excess of the model background mixture at final concentrations of 1% and 4% by DNA mass, respectively. The DNA was extracted, purified, digested, and tagged using a standard sample preparation protocol, and the entire sample containing 10 ng of DNA was processed on LOC-DLA.

The single molecule classification of the resulting data from DLA demonstrated confident detection of both *E. coli* and *S. epidermidis*, as well as two additional components of the complex background: *F. johnsoniae* and *V. fischeri* (Fig. 5). Several genomic fragments of each bacterium were reliably detected (Fig. 5a). The detection confidence varied for different fragments, depending primarily on the "uniqueness" of the pattern generated by a fragment. Two *S. epidermidis* fragments with long length and rich patterns demonstrated an extremely high confidence of detection with *p*-values below 10^{-16}. Because the restriction enzyme and the probe were optimized for specific target detection, the proportion of detected *E. coli* fragments was highest even though it was a minor component of the mixture. Several background bacteria had GC-rich genomes, which were selectively degraded to very small fragments by using the ApaI restriction enzyme with the recognition sequence GGGCCC. These fragments were rejected by the DNA prism and therefore were not measured, thus increasing the detection efficiency for the targets of interest.

The potential to identify multiple fragments from each bacterial genome increases the confidence of detecting a target of interest. This is represented by the Total Log-Likelihood (TLL) metrics (Fig. 5b, see ESI† for details). In this experiment, observed DNA fragments were compared against a pattern database including 98 DNA fragments ranging in length from 160 to 300 kb. These represent a test library of 40 different strains from 22 distinct species. In Fig. 5b, only the 15 bacteria from the database that generated "hits" against the detected fragments are presented. *E. coli, S. epidermidis, F. johnsoniae*, and *V. fischeri* all had significantly higher TLL than all other potential hits; no other organism in the database appeared as a significant false-positive detection event. Other components of the complex biological background sample were not included in the test database, and therefore were not detected in this experiment.

The example presented here is a representative of hundreds of repeated operations of the LOC-DLA system under a variety of test samples and conditions. In integrated operation with the sample preparation reactor, LOC-DLA could be used to consistently detect DNA fragments from 5×10^3 target cells in a mixture of 6×10^4 to 6×10^6 background organisms (data not shown).

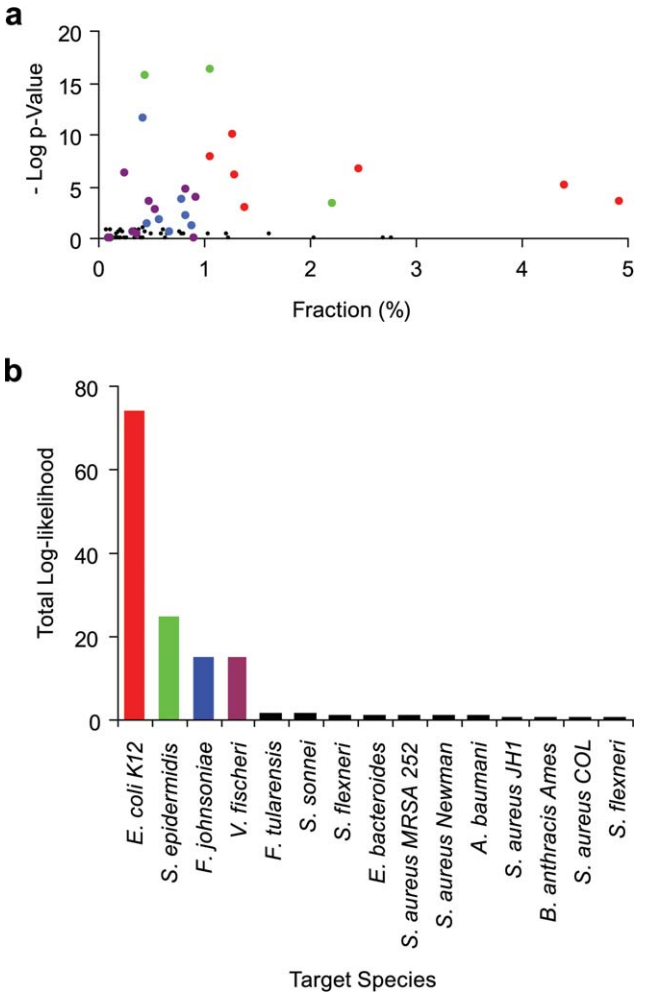

Fig. 5 Detection of a target microbe at low concentration in a complex bacterial mixture. The targets, *E. coli* and *S. epidermidis*, were present at 1 and 4% by DNA mass, respectively. (a) *p*-Value of detection for genomic DNA fragments of various species is depicted *vs.* the relative quantity of molecules attributed to each fragment by classifying software (expressed as a percentage of the total number of analyzed molecules). Each dot corresponds to a DNA fragment of specific length from the DLA range. Smaller *p*-value (higher position on the *Y*-axis) means higher confidence of detection. Only the fragments from the target organisms and the components of the background included in the database exhibit a significant confidence of detection: *E. coli* (red), *S. epidermidis* (green), *F. johnsoniae* (blue), and *V. fischeri* (purple). (b) Total log-likelihood of microbe detection. Only 15 bacteria, which generated "hits" against the detected fragments, are presented.

Digital DNA immunoassay on LOC-DLA

As described previously, LOC-DLA includes the structures required for the multiplex Digital DNA assay, including two stages of sample concentration and detection. Incorporating on-chip concentration allows for electrokinetic transfer of the

prepared DNA from the mini-reactor and minimizes the sample read time by optimizing the sample concentration at the detector. The separate microfluidic structure operates independently from the DLA portion of the device (Fig. 1a, features 1′–6′). The DNA stretching funnels of the DLA and Digital DNA sections of the device are arranged in an anti-parallel orientation with a 10 μm separation (Fig. 6a). The close proximity of the detection channels allows for simultaneous observation of both channels in a single field of view at 100× magnification and automated positioning of the detection optics when switching from one mode of detection to the other. Operation of the Digital DNA portion of the device is similar to the concentration stages of the DLA device: concentration of the sample to the primary gel bank at 25 μA for 45 min, transfer to the secondary gel bank at 3 μA for 45 min, and elution toward the detection funnel at 1 μA for ~5 min.

As an example of Digital DNA performance, positive detection of 167 fmol (25 pg) botulinum toxoid has been demonstrated on the LOC-DLA platform (Fig. 6b and c). Digital DNA was prepared as described previously.[8] The engineered 85 kb DNA molecule consists of a series of eight binary sections that either bind or do not bind fluorescent labeled bisPNA tags. These bisPNAs also carry recognition antibodies specific for the target of interest. Combinations of different binary sequences, with different recognition antibodies, allow for massive multiplexing of Digital DNA assays.[8]

The purified Digital DNA was intercalated with POPO-1 and hybridized with fluorescently labeled bisPNA. The Digital DNA was also incubated with the target of interest, botulinum toxoid, and a secondary antibody fluorescently labeled in a third color. This created a sandwich immunoassay, with toxoid bound to both the Digital DNA and to a signal antibody. The sample was loaded and run on LOC-DLA as described. Fig. 6b shows the distribution of different length DNA molecules detected in this sample. Uniformly stretched Digital DNA appears as a punctate cluster near 25 μm. Similarly to the engineered DNA used for the DNA prism assessment, the Digital DNA sample was also prepared using the Qiagen Maxiprep kit[8] and therefore included short fragments, as seen as a triangular wedge of under stretched molecules near the origin in this plot.

Analysis of the tag fluorescence patterns indicates detection of the botulinum toxoid. The Digital DNA assay forms an antibody–antigen–antibody sandwich, where both antibodies are conjugated to fluorophores in two distinct colors. As a result, in the case of successful detection using DLA stretching fluidics, the secondary antibodies bound through the targets and primary antibodies to bisPNAs generate a pattern (red) similar to the one generated by the identification of bisPNAs (green).[8] Therefore, the presence of the red trace and its similarity to the green trace in Fig. 6c are the signs of positive detection of botulinum toxoid.

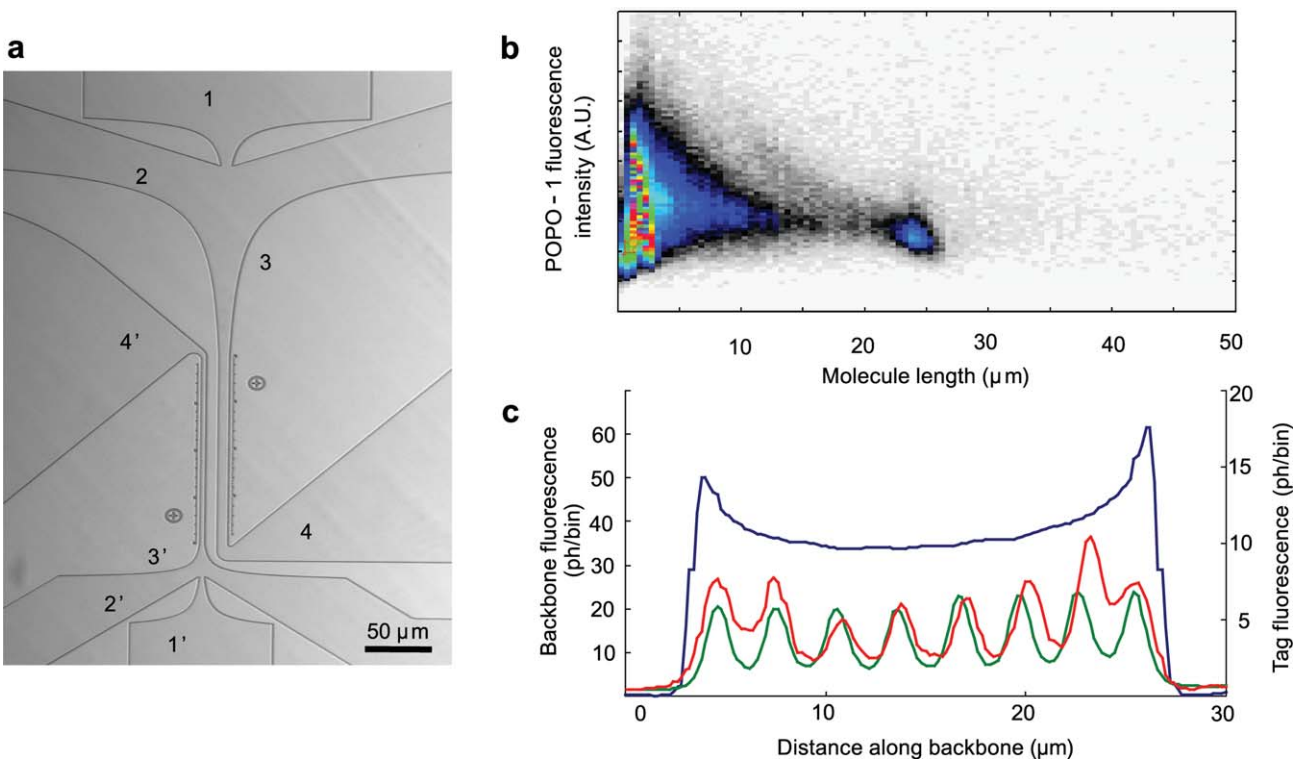

Fig. 6 Digital DNA assay in LOC-DLA. (a) Micrograph of stretching funnel arrangement in LOC-DLA. DLA section: 1, DNA entrance channel; 2, sheath flow channels; 3, stretching funnel and detection channel; 4, waste exit channel. These structures are repeated (1′–4′) in an anti-parallel orientation for the Digital DNA detection section of the device. The funnel geometry for this device is optimized for uniform stretching of 85–125 kb Digital DNA.[8] (b) Molecule distribution of an example sample of 85 kb Digital DNA. The prepared sample included 50 ng of Digital DNA tagged with fluorescent bisPNA and intercalated with POPO-1, 167 nmol (2 ng) botulinum toxoid, and 1 pmol fluorescently labeled anti-toxoid antibody. (c) Average fluorescent signals of multiple Digital DNA units: from backbone-bound intercalator (blue), from hybridized identification tags (green), and from bound anti-toxoid antibodies (red).

Discussion

A biosensor for the detection of airborne pathogens has several requirements: ability to detect a wide range of targets in a complex biological background, high sensitivity, low rate of false-positive identification, and low cost per assay. These requirements are further complicated in that airborne threats include bacterial, viral, and small molecule pathogens, each of which typically requires different detection methodologies. We have presented here a device that integrates Direct Linear Analysis of bacterial mixtures with Digital DNA immunoassays for the detection of viral and small molecule pathogens in a format that meets the stringent requirements of an airborne pathogen detection system.

DLA has several characteristics that make it particularly valuable for bacterial detection and identification. It has the potential to detect a vast variety of organisms using a single unified reagent set. This reduces both time and cost per assay, as no *a priori* knowledge of the target sample is needed, and specific reagents such as oligonucleotide primers or antibodies are unnecessary. Identification of bacterial threats is accomplished by matching the genome-specific fluorescent tagging pattern of individual long fragments of DNA against a library of previously determined traces. A significant advantage of DLA detection therefore is that the library of detectable organisms can be updated electronically, with no requirement for novel chemistry development to add an additional target organism to the test database. This capability makes DLA particularly responsive to tracking novel pathogens that have evolved naturally or been intentionally modified.

DLA is inherently a single molecule classification technique. The sensitivity of detecting a rare target organism in a large excess of background DNA, therefore, requires high throughput of analyzable molecules. The DNA content expected in typical air sample is small and variable (expected in the range of 0.05–5 ng).[18–21] The sample of prepared DNA must therefore be transferred from the reaction chamber efficiently and at high concentration to optimize DLA detection. At low DNA concentrations, DLA detection efficiency suffers because molecules are spaced far apart at the detector, and most of the detection time is spent reading empty solvent. The multistage concentrators on LOC-DLA allow for a significant improvement in the occupancy of DNA at the detector. At high DNA concentrations, however, molecules become so closely spaced that the majority arrive at the detector overlapped, thus becoming impossible to analyze. The extent of overlapping molecules is highly dependent on the range of molecule lengths present in a given sample (see ESI† for discussion). Selectively removing short fragments (less than 150 kb) from the sample reduces the frequency of overlapping molecules, allowing DLA detection at higher efficiency. Moreover, as detection of a target does not require the measurement of the whole genome, keeping only a few sufficiently long DNA fragments also reduces the time of measurement. This effect further helps to reduce the influence of the biobackground because some of the admixture microbes are shredded into short pieces by the restriction enzyme optimized to extract long fragments from target microbes.

We have explored two alternative approaches to increasing molecule throughput in DLA detection. First, we have explored performing measurements simultaneously through several parallel fluidic channels. Second, we have attempted to increase the speed of the molecules through a single channel. Both solutions pose technical difficulties. The former approach requires multiple detection zones, complicating the optical arrangement of excitation lasers and detection hardware. The latter approach requires redesign of stretching geometry to prevent overstretching of long molecules at high velocities and to avoid a considerable increase in the driving pressure.[14] Also the increased velocity of the molecule movement through the detection zone reduces the number of detected photons from DNA-bound fluorophores, reducing in turn the ability to identify and classify DNA fragments. We plan to present these approaches in future publications.

The incorporation of the Digital DNA multiplex assay expands the system's ability to identify a broad spectrum of targets by the inclusion of non-cellular pathogens. This approach is complementary to DLA because it can be performed using the same sample preparation system, uses the same stretching fluidics and the same detection optics. In LOC-DLA, Digital DNA functions are still physically separated from the DLA section. However, we found that fully loaded Digital DNA particles, *i.e.* including the DNA molecule with the bound targets and secondary antibodies, can be carried through all stages of the DLA section without noticeable loss of sensitivity. Moreover, the DNA prism works remarkably well to separate free fluorescent signal units from the assembled Digital DNA sandwich assay, thus providing an improved detector resolution and an enhanced signal-to-noise.[8] Future iterations of LOC-DLA, therefore, will not require a dedicated Digital DNA section at all, processing both DLA and Digital DNA samples through the same structures and simplifying the LOC-DLA design.

The future development of the LOC-DLA integrated system for airborne pathogen involves further improvements to system transfer efficiency, simplification of the chip interface, and optimization of the system as a deployable device. Presently, LOC-DLA can provide sufficient DNA from a 0.5–5 ng sample to accommodate many hours of continuous detection. However, a significant DNA remains throughout the chip after each run. This carryover can be due to residual DNA at the polymer gel surfaces, trapping of DNA in low electric field zones at channel intersections in the chip, and dispersed DNA due to inefficient transfer from the final gel towards the detection funnel. Each of these modes of DNA loss can be rectified through refined polymer gel chemistry, optimized channel geometry, and revised design of the final gel structure, respectively. Presently, the fluidic and electric interface with microfluidic device requires a large number of fluidic connections to be made through fluid-filled Tygon tubes, each of which adds to the risk of trapping air bubbles in the system. In future LOC-DLA systems, the remote fluidic interface wells will be integrated with the manifold, simplifying the connections and minimizing the efforts to maintain and operate the system. Finally, the entire integrated sample collection, preparation, and detection platform will be simplified and automated to yield a robust, fieldable airborne pathogen detection system.

Acknowledgements

This work was supported by the US Department of Homeland Security, Science and Technology Directorate contract

HSHQPA-05-9-0019. We would like to thank Wendy Benbow, David Johnson, Kwan-yu Li, Marcia Caamano, and Kevin Kornelsen for helpful discussions concerning microfabrication processes. We greatly appreciate Victor Mokgakala, Jose Rojas, Alice Gitau, and James AlHussaini for microfluidic device preparation. We are thankful to Douglas Cameron and Niru Chennagiri for their collaboration in development of the classification algorithm for complex mixtures, as well as Sameh El-Difrawy, Henry Park, Martin Deacutis, and David Scott for hardware control and data acquisition software development. Finally, we thank Simranjit Singh, Manav Mehta, Michael Min, Meng Zhang, Chee-Ho Choi, Muriel Mendes, and Michael LaMontagne for sample preparation and technical expertise.

References

1 D. V. Lim, J. M. Simpson, E. A. Kearns and M. F. Kramer, *Clin. Microbiol. Rev.*, 2005, **18**, 583–607.
2 J. Ho, *Anal. Chim. Acta*, 2002, **457**, 125–148.
3 D. M. Olive and P. Bean, *J. Clin. Microbiol.*, 1999, **37**, 1661–1669.
4 E. Protozanova, M. Zhang, E. J. White, E. T. Mollova, D. Ten Broeck, S. V. Fridrikh, D. B. Cameron and R. Gilmanshin, *Anal. Biochem.*, 2010, **402**, 83–90.
5 E. J. White, S. V. Fridrikh, N. Chennagiri, D. B. Cameron, G. P. Gauvin and R. Gilmanshin, *Clin. Chem. (Washington, DC, U. S.)*, 2009, **55**, 2121–2129.
6 Y. W. Tang, *Clin. Chem. (Washington, DC, U. S.)*, 2009, **55**, 2074–2076.
7 L. M. Wein and Y. Liu, *Proc. Natl. Acad. Sci. U. S. A.*, 2005, **102**, 9984–9989.
8 R. E. Burton, E. J. White, T. R. Foss, K. M. Phillips, R. H. Meltzer, N. Kojanian, L. W. Kwok, A. Lim, N. L. Pellerin, N. V. Mamaeva and R. Gilmanshin, *Lab Chip*, 2010, **10**, 843–851.
9 E. T. Mollova, V. A. Patil, E. Protozanova, M. Zhang and R. Gilmanshin, *Anal. Biochem.*, 2009, **391**, 135–143.
10 K. M. Phillips, J. W. Larson, G. R. Yantz, C. M. D'Antoni, M. V. Gallo, K. A. Gillis, N. M. Goncalves, L. A. Neely, S. R. Gullans and R. Gilmanshin, *Nucleic Acids Res.*, 2005, **33**, 5829–5837.
11 A. V. Hatch, A. E. Herr, D. J. Throckmorton, J. S. Brennan and A. K. Singh, *Anal. Chem.*, 2006, **78**, 4976–4984.
12 E. A. Doherty, K. D. Berglund, B. A. Buchholz, I. V. Kourkine, T. M. Przybycien, R. D. Tilton and A. E. Barron, *Electrophoresis*, 2002, **23**, 2766–2776.
13 E. A. Doherty, R. J. Meagher, M. N. Albarghouthi and A. E. Barron, *Electrophoresis*, 2003, **24**, 34–54.
14 J. W. Larson, G. R. Yantz, Q. Zhong, R. Charnas, C. M. D'Antoni, M. V. Gallo, K. A. Gillis, L. A. Neely, K. M. Phillips, G. G. Wong, S. R. Gullans and R. Gilmanshin, *Lab Chip*, 2006, **6**, 1187–1199.
15 F. C. Leinweber, M. Pfafferody, A. Seidel-Morgenstern and U. Tallarek, *Anal. Chem.*, 2005, **77**, 5839–5850.
16 L. R. Huang, J. O. Tegenfeldt, J. J. Kraeft, J. C. Sturm, R. H. Austin and E. C. Cox, *Nat. Biotechnol.*, 2002, **20**, 1048–1051.
17 L. R. Huang, J. O. Tegenfeldt, J. J. Kraeft, J. C. Sturm, R. H. Austin and E. C. Cox, *Tech. Dig. - Int. Electron Devices Meet.*, 2001, 363–366.
18 S. Tringe, T. Zhang, X. Liu, Y. Yu, W. Lee, J. Yap, F. Yao, S. Suan, S. Ing, M. Haynes, F. Rohwer, C. Wei, P. Tan, J. Bristow, E. M. Rubin and Y. Ruan, *PLoS One*, 2008, **3**, e1862.
19 J. Radosevich, W. Wilson, J. Shinn, T. DeSantis and G. Andersen, *Lett. Appl. Microbiol.*, 2002, **34**, 162–167.
20 E. Brodie, T. DeSantis, J. Parker, X. Zubietta, Y. Piceno and G. Andersen, *Proc. Natl. Acad. Sci. U. S. A.*, 2007, **104**, 299–304.
21 N. Fierer, Z. Liu, M. Rodrigues-Hernandez, R. Knight, M. Henn and M. Hernandez, *Appl. Environ. Microbiol.*, 2008, **74**, 200.